Available online at www.sciencedirect.com
ScienceDirect
Journal of the European Ceramic Society 30 (2010) 2183–2189
www.elsevier.com/locate/jeurceramsoc

Non-contact mechanical property measurements at ultrahigh temperatures

Sindhura Gangireddy [a], John W. Halloran [a,*], Zachary N. Wing [b]

[a] University of Michigan, Ann Arbor, MI 48109-2136, USA
[b] Advanced Ceramics Manufacturing, Tucson, AZ 85706-9645, USA

Available online 20 February 2010

Abstract

The "Electro-Magnetic Mechanical Apparatus", a novel non-contact method of mechanical testing of ultrahigh temperature ceramics at high temperatures, was developed where a mechanical stress is applied using Lorenz forces on a sample heated to high temperatures with an electric current. The design of the apparatus and an analysis relating stress to magnetic flux density, electrical current, and specimen dimensions are presented here. Significant creep deformations were observed in ZrB_2–SiC samples deformed under 20 MPa of flexural stress resulting in 0.08% strain after 240 s at 1600 °C and 0.21% strain after 150 s at 1750 °C. A fatigue load of 6 MPa at 60 Hz frequency at 1700 °C in air increased the oxidation rate. This mechanical apparatus has potential application not only for high temperature creep and fatigue experiments but also fracture and elasticity. Though developed for ceramics, this technique can be used to study high temperature mechanical properties of any conducting material.

Keywords: C. Creep; E. Refractories; D. Borides; C. Mechanical properties; ZrB_2

1. Introduction

Extremely refractory materials like UHTC are of interest precisely because they melt at higher temperatures than most other materials.[1] Their mechanical properties are of direct interest at extreme temperatures. However, flexural creep experiments tend to be limited in temperature owing to reaction between fixture and the specimen, which often limits creep data to temperatures ≤1500 °C.[2–4] A flexural creep technique that does not involve contact with a specimen under test could simplify measurements at higher temperatures.

This paper addresses these issues through a non-contact method where the hot specimen is not touched by any fixtures. Current is used to resistively heat thin sections of the specimen. The application of a magnetic field generates electro-magnetic forces that apply stress to the sample. This technique is called the Electro-Magnetic Mechanical Apparatus (EMMA). Thus eliminating any kind of contamination from contact with foreign material at high temperatures, it is possible to achieve mechanical testing at temperatures as high as 1950 °C. The analysis, prototype realization and preliminary results from the Electro-Magnetic Mechanical Apparatus (EMMA) are presented in this paper.

2. Analysis of the Electro-magnetic Mechanical Apparatus

2.1. Relation of stress to current, flux density, and specimen geometry

The EMMA is a modified version of the "ribbon apparatus" for high temperature oxidation of conductive samples,[5] where a thin ribbon, illustrated in Fig. 1A, is heated by an electric current **I** (either direct or alternating) that runs longitudinally down the length of the ribbon. Here we exploit the fact that the current **I** in the ribbon can be easily used to generate a mechanical stress with the electro-magnetic Lorentz force $\mathbf{F} = \mathbf{I} \times \mathbf{B}$, per unit length under a transverse magnetic flux density. If the current is applied in the x-direction along the length of a sample L_T, and the magnetic flux density is applied in the y-direction, there with be a distributed mechanical loading (w in N/m) directed vertically in the z-direction: $w_z = \mathbf{I_x B_y}$. The principles are illustrated in Fig. 1B. For example, if the current is 100 A and the magnetic flux density is 0.5 T (or 0.5 N/mA), there will be a uniform loading $w = 50$ N/m. The total force on a 40 mm long specimen

* Corresponding author at: Materials Science and Engineering Department, University of Michigan, 2300 Hayward Street, 2010 HH Dow, Ann Arbor, MI 48109-2136, USA. Tel.: +1 734 763 1051; fax: +1 734 763 4788.
E-mail address: peterjon@umich.edu (J.W. Halloran).

0955-2219/$ – see front matter © 2010 Elsevier Ltd. All rights reserved.
doi:10.1016/j.jeurceramsoc.2010.01.006

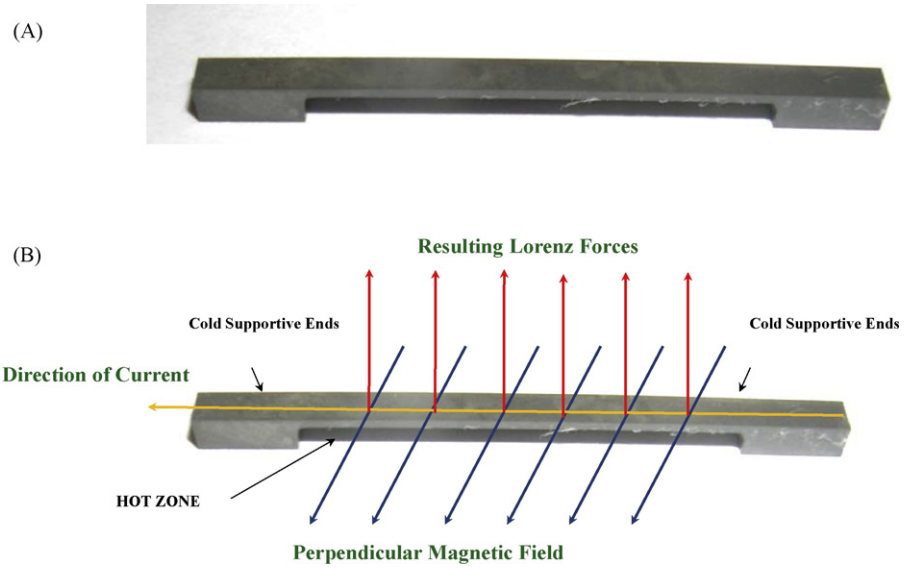

Fig. 1. (A) Ribbon sample made by machining the center of a flexural testing bar to thin ribbon. (B) Axial current **I** and transverse magnetic field **B** create a vertical mechanical force, $\mathbf{F} = \mathbf{I} \times \mathbf{B}$.

($L_T = 0.040$ m) will be 2 N. This is not a large force, so it will be easy to keep this specimen attached to a support structure, but it suffices to create a large stress on thin ribbon section.

The geometry of the UHTC Ribbon Specimen, shown in Fig. 1A, is a small bar specimen such as a standard bar used for flexural testing, with thickness t_T (~2 mm), width Y and total length L_T. The center section of the bar is machined away to leave a ribbon of length L and thickness t (~ 400–500 μm). When an electrical current **I** passes down the length of the specimen, the current density is low in the cold support (current density $= \mathbf{I}/Yt_T$) and it remains cool. But the current density is much higher in the ribbon current density $= \mathbf{I}/Yt$, and heats to incandescence. Thus there is very hot ribbon self-supported by its cold ends. The hot ribbon section is not in physical contact with the rest of the apparatus, so there are no problems with materials compatibility and substrate reaction.

The temperature Θ of the ribbon varies almost parabolicly across the ribbon section,[6] depending on the current **I**, electrical resistivity $\rho(\Theta)$, and heat transfer conditions by conduction, convection, and radiation. This is conveniently measured with a micro-optical pyrometer. To approximately show how the temperature varies with current, we consider very long ribbons in vacuum under conditions where radiation dominates. The temperature varies with current approximately as Eq. (1):

$$\Theta \approx \frac{\beta}{(\rho(\Theta)\varepsilon)^{1/4}}\mathbf{I}^{1/2} \tag{1}$$

where ε is the emissivity and β involves geometric factors such as surface area.[7]

If the entire specimen is exposed to a transverse magnetic flux density $\mathbf{B_y}$, it will experience a uniform distributed mechanical load w_z, as described above. But the section modulus of the specimen changes dramatically in the thin ribbon section, so that if the cold support ends are held in place, the thin ribbon behaves like a beam of length L with fixed ends. This distributed force w_z creates a moment M in the center of the span given by

$$M = w_z\frac{L^2}{24} \tag{2}$$

The ribbon is a beam of width Y and thickness t, with a moment of inertia $Yt^3/12$. The bending moment M creates a tensile stress in the outer fiber of the beam given by[8]

$$\sigma_{max} = \frac{Mc}{I} = \frac{Mt}{2I} = \frac{Mt}{2Yt^3/12} = \frac{w_z L^2}{24}\frac{6}{Yt^2} \tag{3}$$

Since the distributed force $w_z = \mathbf{I_x}\mathbf{B_y}$, the maximum flexural stress on the ribbon is related to the current, magnetic flux, and ribbon dimensions by Eq. (4):

$$\sigma_{max} = 0.25\frac{L^2}{Yt^2}(\mathbf{I_x}\mathbf{B_y}) \tag{4}$$

For a typical case where $\mathbf{I} = 50$ A, and $\mathbf{B} = 0.5$ T (or 0.5 N/A), with a ribbon with $L = 25$ mm, $Y = 2$ mm and $t = 0.2$ mm, the maximum stress is about 50 MPa. This is sufficient to cause significant creep deflection at 1500 °C or above for most ZrB_2–SiC composites, based on recent creep data.[2] A specimen twice as long ($L = 50$ mm), should experience 200 MPa, enough for fracture at high temperature.

The current $\mathbf{I_x}$ cannot be changed without changing the temperature Θ, so in order to vary the stress at constant temperature, either the magnetic flux or specimen dimensions must change. We can approximately model this by using Eq. (1) to express the current as an implicit function of temperature:

$$I \approx \sqrt{\frac{\rho\varepsilon}{\beta}}\Theta^2 \tag{5}$$

which can be substituted into the expression for stress to give,

$$\sigma_{max} \approx 0.25\sqrt{\frac{\rho\varepsilon}{\beta}}\Theta^2\left[\frac{L^2}{Yt^2}\right]B_z \tag{6}$$

This approximately relates the stress to magnetic flux density and the current-dependant temperature. Because the temperature and the stress are both related to current, mechanical properties testing with EMMA would be conducted rather differently than conventional tests, which often are done with independently chosen temperatures and stress levels. The following sections will discuss techniques for conducting non-contact mechanical property evaluations with EMMA, as contrasted with conventional flexural testing methods.

2.2. Mechanical testing methods with EMMA: creep measurements

For conventional creep experiments, one measures the deflection ($\delta(t)$) of a specimen during creep as a function of time at constant temperature, with emphasis on Stage II or "steady state" creep, when the creep rate is constant with time. The stress dependence is found by varying applied stress in the steady state regime, measuring deflection rate vs. stress. Temperature dependence is done by a series of isothermal experiments to discover the steady state creep rate vs. temperature. Typically one has repeated specimens at a limited number of temperatures, so that the creep rate is established rather well, but only at a few discrete temperatures. With EMMA, the Lorenz force and temperature are both depend upon current, so applied stress and temperature cannot be independently varied. Isothermal experiments where one measures creep deflection vs. time vs. applied stress at constant temperature are rather inconvenient, unless $\mathbf{I_x}$ can be held constant and the magnetic flux $\mathbf{B}$ is varied, or specimen geometry is varied. It may prove more convenient to explore creep as a function of current and record creep deflection and temperature as *dependent variables*. Thus the creep rate at low-current will be slow (since temperature is lower and stress is lower), but creep rate will be rapid at higher current (since both temperature and stress are higher). A series of observations of creep deflection δ for various exposure times τ at particular values of current $\mathbf{I}$, with measurements of the temperature Θ should provide the complete description of the creep rate

$$\varepsilon \approx \frac{\Delta\varepsilon}{\tau} \cong A\ \exp\left(\frac{-Q}{R\Theta}\right)\sigma^n \tag{7}$$

This would be simpler if the stress exponent, $n = 1$ (as is approximately the case for ZrB_2–SiC[2]), but a sufficient set of $\{\delta, \tau, \Theta\}$ measurements for a variety of $\{\mathbf{I}, \mathbf{B}, \tau\}$ parameters should be able to provide the creep exponent and activation energy. It will be possible to get many sets of $\{\delta, \tau, \Theta\}$ measurements at various stress/temperature conditions from a single specimen, by measuring deflection after different exposures to current. A single specimen can provide many points of creep rate, stress, and temperature, allowing the creep behavior to be economically mapped. Perhaps the creep rate would not be accurately known at any one temperature (compared to conventional tests), but there would be many more temperature values (rather than just a few). When a specimen eventually breaks, the stress–strain–temperature condition provides a data point for creep-fracture behavior.

2.3. Mechanical testing methods with EMMA: fast fracture

The conventional method to determine strength vs. temperature is to conduct a series of isothermal fracture tests, where a set of specimens is fractured and the fracture strengths recorded as σ_f. Temperature dependence is obtained by running a set of tests at a few discrete temperatures. Since fracture strength tends to be scattered, a large data set is needed for each temperature. This consumes many specimens and time since the sample and fixture typically needs to be heated and cooled for each strength point. Sometimes, one attempts to discover the Wiebull parameters characterizing the strength distribution for each temperature, which is costly and tedious. Conventional strength data tend to be easier to obtain at lower temperatures (where it is less interesting), and increasingly difficult to obtain at very high temperatures (where it is most interesting), for the practical reason that very high temperature strength measurements are challenging and expensive.

With EMMA, it might be more convenient to select a number of magnetic flux values $\mathbf{B}$ and sample geometries (L^2/Yt^2) and increase current until the sample fractures, recording the measured temperature at fracture Θ_f and the calculated stress at fracture σ_f. With multiple samples, one maps out the strength vs. temperature behavior with multiple $\{\sigma_f, \Theta_f\}$ points, one from each specimen for each value of magnetic flux and sample geometry. The scatter in the $\{\sigma_f, \Theta_f\}$ surface contains the Weibull information, which might be extractable by deconvolution. The EMMA method emphasizes very high temperatures, and would make strength data more common for higher temperatures, and less common for lower temperatures, so it provides a very good compliment for the conventional method.

2.4. Mechanical testing methods with EMMA: cyclic fatigue

Cyclic fatigue is conventionally done by seeking the S–N–Θ surface, defining cycles to failure (N_f) as a function of applied stress (S) and temperature Θ. The conventional method determines N_f at several discrete levels of stress at several discrete temperatures. Cyclic fatigue experiments are tedious and expensive. With the EMMA method, fatigue experiments can be accomplished most easily using a constant magnetic flux and an AC electrical current. For example, an ordinary 60 Hz AC current would produce 10^5 fully reversed stress cycles in about 28 min. A set of experiments at constant current, for a particular value of magnetic flux $\mathbf{B}$ and sample geometries (L^2/Yt^2), will determine the N_f from the time it takes to fracture a specimen at constant S and Θ. With a different set of $\mathbf{B}$ and/or geometry, one gets N_f at another value of S for a given temperature. It might be possible to map out the S–N–Θ with fewer specimens in a shorter time.

2.5. Mechanical testing methods with EMMA: elastic modulus and mechanical damping

Much can be inferred from the real part, the complex modulus E' (storage modulus or Young's modulus) and the imaginary part

of the complex modulus E'' (loss modulus for mechanical damping), since the Young's modulus is itself a critical property while the loss modulus reports the high frequency creep/plasticity behavior. This can be easily measured by the standard impulse excitation technique, using electro-magnetic impulse created by quickly moving a small but powerful permanent magnet near the hot ribbon. During the brief transit of the magnet, the sample will experience a pulsed magnetic flux, which creates a transient force that will excite vibrations of the ribbon. These vibrations could be detected remotely with a laser vibrometer, or with an acoustic microphone pickup, which can be interpreted with standard commercial software. From the vibration frequency, one infers the storage modulus E' and the loss modulus E'' is inferred from the damping of the vibration.

3. Realization of a prototype Electro-Magnetic Mechanical Apparatus

To demonstrate the principal of EMMA, we have used rather simple, low cost components in the laboratory, since we envision EMMA to be a compact tabletop device. The apparatus has two essential elements: (1) controllable electrical current, with fast feedback so that temperature can be controlled; (2) a means to expose the sample to a magnetic flux density on the order of 0.3–0.5 T. A DC power supply [Sorensen SGI 100–150] provides a current of 30–100 A at a relatively low voltage (about 1 V) to heat the sample and create a constant Lorentz force. Permanent magnets are used to provide the magnetic flux, rather than electromagnets, since the latter are costly and quite bulky. Two powerful neodymium boron iron block-shaped magnets are opposed *N*–*S* vs. *N*–*S*, with a controlled air gap between them so that the magnetic flux density can be changed by changing the air gap. The magnetic circuit is completed with an iron path. The Nd–Fe–B permanent magnets (Grade N52, K&J Magnetics, Jamison PA USA) have dimensions 50.8 mm long by 25.4 mm wide, by 12.7 mm thick, and produce a surface field of 0.6325 T. The attractive force between the two magnets is nearly 1780 N, so the fixture must be robust.

The apparatus is illustrated in Figs. 2 and 3, with the modification made to the ribbon method. Fig. 2 is a top view of the ribbon apparatus inside the magnetic flux assembly. It shows a ZrB_2–SiC ribbon specimen (grey) attached to a current conductive plate, which supplies the current from the power supply via the current leads to either side. The specimen is held onto the conductive plate with a spring clip, which exerts just enough force for good electrical contact. Passing a modest current (~50 A) suffices to heat these ribbons to temperatures in the 1400–2000+ °C range in the open air.

Fig. 3 is a photograph of the magnetic flux assembly (MFA). Due to the strong attractive force between the magnets, we attach the magnets with brass fixtures to thick steel blocks held securely by a machinists vise. The brass fixture is a magnetically transparent means to hold the block magnets to the plate against the rather strong attractive force, and a high thermal conductivity sink for heat radiated from the hot specimen to prevent the Nd–Fe–B from getting hot. Magnetic flux density varies as a function of air gap and can be adjusted easily by moving the vise jaws. The vise also serves as a high permeability iron path for the magnetic circuit.

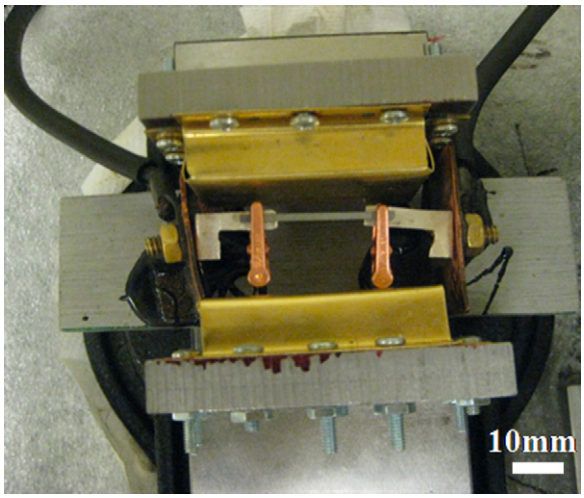

Fig. 2. The ribbon specimen (center grey feature) held on the current leads (L-shaped silver features) with alligator clips, within the air gap between two Nd–Fe–B permanent magnets (held in brass box).

The complete Electro-Magnetic Mechanical Apparatus (EMMA) system is shown in Fig. 4. This shows the self-heating ribbon in the magnetic flux assembly resting on the bench top, with a micro-pyrometer above the hot ribbon supported by a lab jack. Not shown is an optical stereomicroscope, used to observe the hot sample during a test. Fig. 5 shows a creep test in operation with the room lights on and off, to illustrate the incandescent hot sample. Notice that UHTC ribbon is at 1750 °C, but the surrounding apparatus is not hot. The cold ends of the sample are held on with copper clips, the current leads have plastic insulation, and the Nd–Fe–B magnets in their brass holders stay at room temperature, even though they are a few millimeters away from the hot ribbon. This is possible because the ribbon is small, so the heat load is only about 100 W.

3.1. Experimental procedure for creep tests

Two ZrB_2–SiC composites were prepared as test samples with the compositions shown in Table 1. Raw materials were

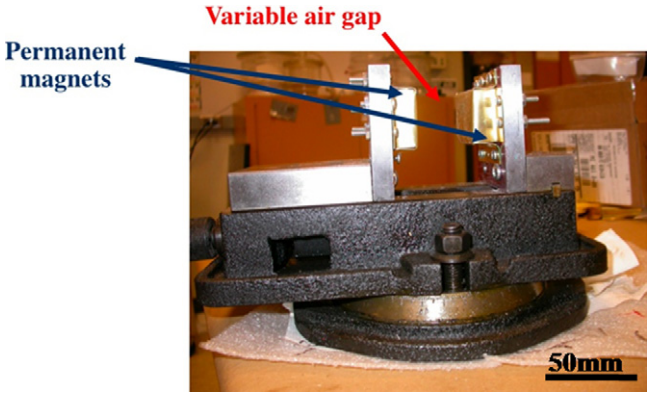

Fig. 3. The magnetic flux assembly, consisting of a brass fixtures holding blocks of Nd–Fe–B magnets, with a vise to achieve a variable air gap.

Fig. 4. Electro-Magnetic Mechanical Testing Apparatus (EMMA) system, showing the self-heating ribbon in the magnetic flux assembly on the benchtop, with the pyrometer above the hot ribbon.

Table 1
Compositions of ZrB_2–SiC composites.

	ZrB_2	SiC	Y_2O_3
Composition 1 (vol%)	68	29	3
Composition 2 (vol%)	70	30	0

obtained from commercial sources: ZrB_2 (HC Stark Grade B), SiC (H.C. Stark Grade UF10), and Y_2O_3 (H.C. Stark Grade C). Powders were ball milled in isopropyl alcohol for 24 h using WC milling media. Powders were dried in a convection oven and sieved prior to firing. The composition of the composite

Fig. 6. ZrB_2–SiC specimen after a creep experiment at 0.34 T magnetic flux density and 36 A current, corresponding to tensile stress of 20 MPa at 1750 °C, showing a creep deflection of 3 mm for about ~0.21% creep strain after 240 s.

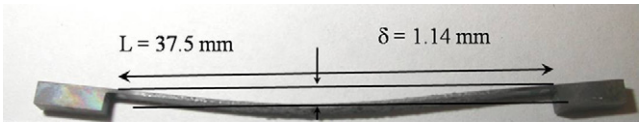

Fig. 7. ZrB_2–SiC specimen after a creep experiment at 0.34 T magnetic flux density and 36–38 A current, corresponding to tensile stress of 20 MPa at 1600 °C, showing a deflection of 1.1 mm for abut ~0.08% creep strain after 150 s.

used for mechanical testing is 68 vol% ZrB_2, 29 vol% SiC and 3 vol% Y_2O_3. Samples were fired in a resistively heated, uniaxial, graphite hot press at 2100 °C in vacuum of ~11 Pa, using a heating rate of 5 °C/min, a pressure of 28 MPa, and a soak time of 30 min. EMMA test bars were abrasively machined to size, while maintaining the neutral axis of bar perpendicular to the compaction axis during firing. Samples were rough machined using a 100 grit diamond wheel and finished to size using a 380 grit diamond wheel.

4. Results and discussion

A limited number of creep experiments were done to demonstrate the EMMA technique. These were done for fixed conditions of temperature, stress and time. The deflections of the specimens after creep were measured at room temperature after the test. Fig. 6 shows a ZrB_2–SiC specimen after 240 s in the apparatus. The magnetic flux density, calculated from the air gap of 9 mm on one side and 18 mm on the other, was 0.34 T. A DC current of 36 A heated the sample to 1750 °C (varying ±30 °C during the test) and created a Lorentz force of 12.2 N/m over the 37.5 mm span, producing a flexural stress of 20 MPa, calculated from the specimen dimensions using Eq. (4). The permanent creep deflection of the sample was $\delta \sim 3$ mm, corresponding to about 0.21% flexural strain. A specimen tested at 1600 °C is shown in Fig. 7. This was exposed 150 s to a 0.34 T flux density, with a DC current of 37 ± 1 A, which for these spec-

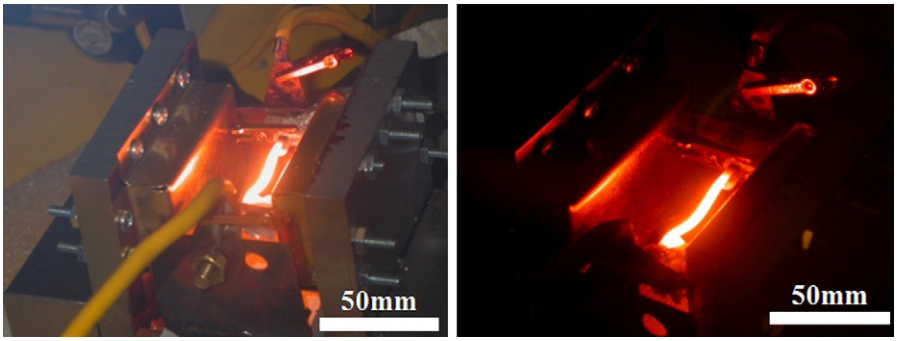

Fig. 5. Left: room lights on; right: room lights off. Creep test for ZrB_2–SiC specimen at 1750 °C. This sample is heated using 36 A DC current, with magnetic flux density 0.34 T. The flexural tensile stress in the ribbon is 20 MPa. Creep deflection of the ribbon is visually obvious.

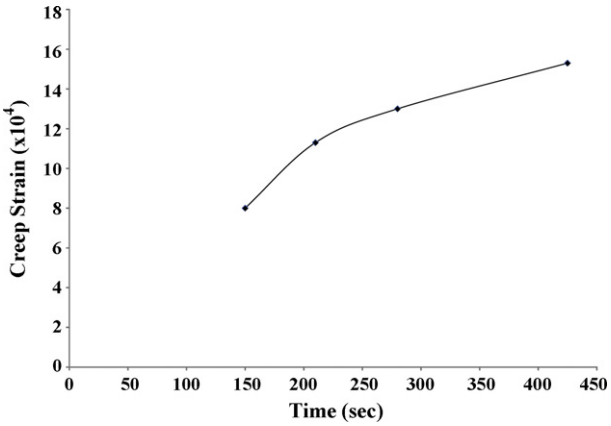

Fig. 8. Creep strain as a function of time for 1600 °C at 20 ± 1.6 MPa stress.

imen dimensions resulted in a temperature of 1600 ± 20 °C and a stress of 20 MPa. The deflection was $\delta \sim 1.1$ mm, corresponding to about 0.08% creep strain. Note that the "cold ends" are no longer co-planar, suggesting there was residual stress relaxation after the ribbon was released. Fig. 8 shows creep strain vs. time for a series conducted at 1600 °C at 20 MPa. The creep rate from this test could be calculated to be $\sim 5 \times 10^{-6}\ s^{-1}$, where as the creep rate extrapolated from the data of earlier researchers of 50% SiC composite, to 1600 °C (which was higher than the existing data) and to 20 MPa (our stress requirement was lower than the data range) was $\sim 1 \times 10^{-6}\ s^{-1}$.[2] This shows the creep rates achieved by EMMA are of the same order as those achieved by conventional testing.

We will not attempt to analyze the time dependence of creep because the data set is limited and these EMMA experiments are conducted in air, so oxidative processes accompany the creep and significant and variable amount of the specimens were consumed by oxidation during the creep test. Unlike conventional creep experiments, where the stressed volume of the specimen is large compared to oxidation-affected zone, the oxidative recession of the ZrB_2–SiC in the ribbon samples can be a significant fraction of the specimen cross-section.

Talmy et al.[2] reported a significant difference in the extent of oxidation on the tensile and compressive sides of their flexural creep specimens. Oxidative creep could be different from simple mechanical creep in these materials, and that oxidation under stress could vary from what would be expected for unstrained materials. This suggests a future series of experiments where oxidation could be avoided, by using a protective atmosphere in a simple enclosure. As this paper concerns the EMMA method and is not about the creep behavior of this particular ZrB_2–SiC composite, we will not address this issue here. We have also conducted very preliminary fatigue experiments with AC current instead of DC current. This produces which produces fatigue condition with fully reversed stress. One sample was rapidly heated to 1700 °C in a magnetic flux density of 0.34 T, with the peak stress of 6 MPa, as calculated with this current and the relevant specimen dimensions, at a frequency of 60 Hz. This specimen failed by oxidative burn-through after 80 s exposure, which corresponds to 4800 stress cycles. A similar sample was heated at the same temperature without the magnetic field, so there was no applied stress. For this unstressed sample, oxidative burn-through occurred after 1080 s. Apparently the oxidation rate is much more severe in the presence of this small cyclic stress.

How does EMMA compare with conventional flexural testing, which used a refractory flexural fixture in a high temperature furnace, with a universal testing machine to apply forces and measure displacements? One advantage of EMMA is that no universal testing machine is needed, since the loads are applied using electro-magnetic forces. This prototype of EMMA did not have a means to measure deflection, but a non-contact deflectometer could be added. However the magnetic flux density and current limit the range of loads. Changing the current changes both temperature and stress, so that the testing protocols will be different. Also EMMA is a novel method, so it is necessary to demonstrate that the results are as reliable as standard methods. A further advantage is that the sample is self-heated and the hot section is self-supported. No refractory fixture is required, and reaction of the sample with the fixture is avoided. But EMMA can only test electrically conductive materials, and the stressed volume is limited to the thin ribbon. Specimen section size effects are anticipated, so that EMMA strengths and creep rates may well be different from conventional standard test specimens. The samples in this prototype of EMMA were exposed to air. Typically creep is done in a protective atmosphere, so this feature should be included in a future version of EMMA.

5. Conclusions

A simple tabletop apparatus can be used to for non-contact mechanical testing at very high temperature for electrically heated conductive materials using the Lorentz force generated by exposing the sample to a magnetic flux density. The technique eliminates problems associated with reaction of the specimen at high temperatures from contact with foreign material. This Electro-Magnetic Mechanical Apparatus (EMMA) was realized using a modified ribbon heating device, and demonstrated with zirconium diorite–silicon carbide at temperatures as high as 1750 °C. Significant creep deflection was observed. The creep rates were found in close agreement to the extrapolated values from conventional testing at lower temperatures. This method can be further applied for high temperature creep, fracture, and fatigue. The ribbon sample is exposed to air for these experiments, but it could easily be enclosed in a protective atmosphere to conduct experiments in controlled environment conditions.

Test variables in EMMA, like temperature and stress, are not independent but mutually dependent on the current value. As a result varying these parameters is not simple, but needs careful adjustment of magnetic field on the specimen (and hence the distance of separation between the magnets and the location of the specimen within this gap).

Acknowledgements

The United States Air Force Office of Scientific Research under Contract FA9550-09-C-0039 supported the development

of EMMA and the Office of Naval Research under grant N00014-02-1-0034 supported the development of the Ribbon Apparatus. We thank Professor Diann Brei of the University of Michigan for the use of her DC power supply.

References

1. Fahrenholtz WG, Hilmas GE, Talmy IG, Zaykoski JA. Refractory diborides of zirconium and hafnium. *J Am Ceram Soc* 2007;**90**(5):1347–64.
2. Talmy IG, Zaykoski JA, Martin CA. Flexural creep deformation of ZrB_2/SiC ceramics in oxidizing atmosphere. *J Am Ceram Soc* 2008;**91**:1441–7.
3. Melendez-Martinez JJ, Dominguez-Rodriguez A, Montervede F, Melandri C, De Portu G. Characterization and high temperature mechanical properties of zirconium boride-based materials. *J Eur Ceram Soc* 2002;**22**: 2543–9.
4. Opeka MM, Talmy IG, Wuchina EJ, Zaykoski JA, Causey SJ. Mechanical, thermal and oxidation properties of refractory hafnium and zirconium compounds. *J Eur Ceram Soc* 1999;**19**:2405–14.
5. Karlsdottir SN, Halloran JW. Rapid characterization of ultra-high temperature ceramics. *J Am Ceram Soc* 2007;**90**:3233–8.
6. Karlsdottir SN. Oxidation behavior of zirconium diboride–silicon carbide composites at high temperatures. PhD Thesis, University of Michigan, Ann Arbor, 2007.
7. Carlsaw HS, Jaeger JC. *Conduction of heat in solids*. 2nd edition Oxford: Oxford University Press; 1959. p. 154–60.
8. Popov EP. *Introduction to mechanics of solids*. Englewood Cliffs (NJ): Prentice-Hall Inc.; 1968. p. 181.